NASA/TM–2011-216420

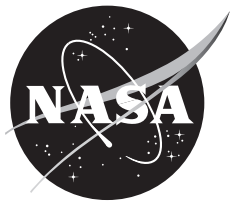

Initiation of Long-Wave Instability of Vortex Pairs at Cruise Altitudes

Vernon J. Rossow
Ames Research Center
Moffett Field, California

February 2011

The NASA STI Program Office . . . in Profile

Since its founding, NASA has been dedicated to the advancement of aeronautics and space science. The NASA Scientific and Technical Information (STI) Program Office plays a key part in helping NASA maintain this important role.

The NASA STI Program Office is operated by Langley Research Center, the Lead Center for NASA's scientific and technical information. The NASA STI Program Office provides access to the NASA STI Database, the largest collection of aeronautical and space science STI in the world. The Program Office is also NASA's institutional mechanism for disseminating the results of its research and development activities. These results are published by NASA in the NASA STI Report Series, which includes the following report types:

- TECHNICAL PUBLICATION. Reports of completed research or a major significant phase of research that present the results of NASA programs and include extensive data or theoretical analysis. Includes compilations of significant scientific and technical data and information deemed to be of continuing reference value. NASA's counterpart of peer-reviewed formal professional papers but has less stringent limitations on manuscript length and extent of graphic presentations.

- TECHNICAL MEMORANDUM. Scientific and technical findings that are preliminary or of specialized interest, e.g., quick release reports, working papers, and bibliographies that contain minimal annotation. Does not contain extensive analysis.

- CONTRACTOR REPORT. Scientific and technical findings by NASA-sponsored contractors and grantees.

- CONFERENCE PUBLICATION. Collected papers from scientific and technical conferences, symposia, seminars, or other meetings sponsored or cosponsored by NASA.

- SPECIAL PUBLICATION. Scientific, technical, or historical information from NASA programs, projects, and missions, often concerned with subjects having substantial public interest.

- TECHNICAL TRANSLATION. English-language translations of foreign scientific and technical material pertinent to NASA's mission.

Specialized services that complement the STI Program Office's diverse offerings include creating custom thesauri, building customized databases, organizing and publishing research results . . . even providing videos.

For more information about the NASA STI Program Office, see the following:

- Access the NASA STI Program Home Page at *http://www.sti.nasa.gov*

- E-mail your question via the Internet to help@sti.nasa.gov

- Fax your question to the NASA Access Help Desk at (301) 621-0134

- Telephone the NASA Access Help Desk at (301) 621-0390

- Write to:
  NASA Access Help Desk
  NASA Center for AeroSpace Information
  7115 Standard Drive
  Hanover, MD 21076-1320

NASA/TM–2011-216420

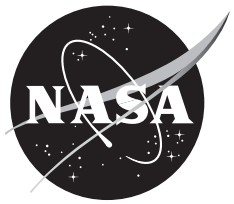

Initiation of Long-Wave Instability of Vortex Pairs at Cruise Altitudes

Vernon J. Rossow
Ames Research Center
Moffett Field, California

National Aeronautics and
Space Administration

Ames Research Center
Moffett Field, California 94035-1000

February 2011

Available from:

NASA Center for AeroSpace Information
7115 Standard Drive
Hanover, MD 21076-1320
(301) 621-0390

National Technical Information Service
5285 Port Royal Road
Springfield, VA 22161
(703) 487-4650

TABLE OF CONTENTS

LIST OF FIGURES

NOMENCLATURE

AR	b^2/S
b	wingspan, ft (m)
b’	spanwise distance between vortex centers, ft (m)
C_L	$L/q_\infty S$
L	$\rho_\infty U_\infty \lvert\Gamma_o\rvert$ b’, lb (N)
q_∞	$\rho_\infty U_\infty^2/2$, lb/ft^2 (N/m^2)
S	wing planform area, ft^2 (m^2)
t	time, s
y, z	distance in lateral and vertical directions, ft (m)
u, v, w	velocity components in x, y, and z directions, ft/s (m/s)
U_∞	velocity of wake-generating aircraft, ft/s (m/s)
Γ	circulation bound in wing, ft^2/sec (m^2/s)
λ	wavelength, ft (m)
ρ	air density, slugs/ft^3 (kg/m^3)
$(\varepsilon\, b')^{1/3}/w_{pr}$	Crow-Bate turbulence parameter
τ	$t_{Link} w_{pr}/b'$

Subscripts

fil	vortex filament
g	wake-generating aircraft
Link	time to vortex linking
o	reference quantity
pr	vortex pair
∞	free-stream condition

INITIATION OF LONG-WAVE INSTABILITY OF VORTEX PAIRS AT CRUISE ALTITUDES

Vernon J. Rossow[1]

Ames Research Center

SUMMARY

Previous studies have usually attributed the initiation of the long-wave instability of a vortex pair to turbulence in the atmosphere or in the wake of the aircraft. The purpose here is to show by use of observations and photographs of condensation trails shed by aircraft at cruise altitudes that another initiating mechanism is not only possible but is usually the mechanism that initiates the long-wave instability at cruise altitudes. The alternate initiating mechanism comes about when engine thrust is robust enough to form an array of circumferential vortices around each jet-engine–exhaust stream. In those cases, initiation begins when the vortex sheet shed by the wing has rolled up into a vortex pair and descended to the vicinity of the inside bottom of the combined shear-layer vortex arrays. It is the in-and-out (up and down) velocity field between sequential circumferential vortices near the bottom of the array that then impresses disturbance waves on the lift-generated vortex pair that initiate the long-wave instability. A time adjustment to the Crow and Bate estimate for vortex linking is then derived for cases when thrust-based linking occurs.

I. INTRODUCTION

The mutually induced or long-wave instability of a vortex pair (refs. 1–3) is generally recognized as the aerodynamic mechanism that most rapidly decomposes the organized flow field of lift-generated vortex wakes. Unfortunately, the instability is not self-starting but requires that a sequence of wave-like in-phase disturbances be impressed along the pair of lift-generated vortex filaments to initiate the process. When the dynamics of the instability was first derived, it was assumed that the instability was initiated by ambient turbulence in the atmosphere. Analysis showed that more intense levels of turbulence in the atmosphere would produce more rapid growth in the amplitude of the disturbance waves and thereby require less time to complete the decomposition of lift-generated vortex wakes. An overview presented in the appendix summarizes experimental studies carried out in water tow tanks that confirm the analysis of Crow (ref. 1) and Crow and Bate (ref. 3) when the instability is initiated by ambient turbulence or by artificially generated disturbance waves (refs. 3–11).

[1] Aviation Systems Division, Ames Research Center, Moffett Field, CA 94035-1000.

The discovery and analysis of the long-wave instability was of immediate interest to airport managers and to the operators of subsonic transport aircraft because persistence of the wakes of preceding aircraft was (and still is) the primary limiting impediment to airport capacity. Research that followed was directed at improved understanding of the instability and at finding other, more rapid ways to initiate the instability. It was hoped that a mechanism could be found that would decrease the time needed for the instability to do its work of decomposition, or that would decrease the hazard posed by the vortex wakes shed by larger aircraft in the transport fleet (refs. 4–28). Studies were also conducted on how best to measure the turbulent structure of the atmosphere and on how best to relate the measurements to the parameters that control the initiation and growth of the long-wave instability (refs. 29–37).

The foregoing studies were informative but did not find a way to use the instability so that it would solve the airport capacity problem, largely because the research did not find a satisfactory initiating solution. The effort did, however, provide much information about the characteristics of the instability. For example, the research efforts showed that, in addition to atmospheric turbulence, the long-wave instability could also be initiated by pitching motions (refs. 1–3 and 6), by roll-oscillation motions (refs. 10 and 11), or by special flap arrangements on the wake-generating aircraft (refs. 5–16). It was also found that a given wake-alleviation procedure could be successful on some aircraft but not on others. For example, roll oscillations were very effective in initiating the long-wave instability to thereby quickly reduce the wake hazard posed by the Boeing B-747 (refs. 10, 11, and 16). However, the same roll-oscillation maneuver did not induce the instability in the wake of the Lockheed L-1011, but substantially increased the magnitude and the duration of the hazard posed by the wake.

The research described herein was developed as part of a continuing effort by the author to use condensation trails behind aircraft at cruise altitudes to observe and study the time-dependent structure of lift-generated vortex wakes (ref. 17). The effort is directed at a search for useable methods for rapid reduction in the hazard level posed by vortex wakes and for improved prediction methods for the time-dependent size of the hazardous region (refs. 37–41). This paper reports on observations of condensation trails of aircraft at cruise altitudes to determine how vortex wakes decompose and spread as a function of time when engine thrust is robust. The observations described indicate that robust thrust levels used by aircraft during cruise cause the long-wave instability to be initiated by a thrust-based mechanism. Supporting computations show that the exhaust streams from the jet engines are redistributed from just below the generating aircraft and near its centerline to the regions around the sides and on top of the lift-generated vortex pair (ref. 42). In this way, the exhaust streams appear to produce an insulating layer of exhaust products between the lift-generated vortex pair and any ambient turbulence that may be in the atmosphere. That is, when engine thrust is robust, it is theorized that ambient turbulence must be very severe in amplitude if it is to initiate waves on the lift-generated vortex pair. Therefore, it appears likely that the products of robust engine thrust may move such that they shield the vortex pair from atmospheric turbulence. If the long-wave instability is to be initiated, it needs to be exposed to some other form of disturbance waves. It is important to note that, like other alternative initiation methods, once initiated, the remainder of the time-dependent dynamics of the long-wave instability is the same as postulated by Crow (ref. 1).

This paper first briefly describes the thrust-based initiation process for the long-wave instability when jet-engine thrust is robust. It then uses observations and photographs of condensation trails to describe the development of the long-wave instability from just after aircraft passage to when wakes become benign. It provides an estimate for the extra time needed for the thrust-based initiation waves to develop and bring about linking between the two vortices in the lift-generated pair. An appendix then presents an overview of water tow-tank experiments that confirm the reliability of the Crow-Bate prediction method when the long-wave instability is initiated by ambient turbulence in the atmosphere (refs. 1–3 and 19–28]. The two wave-initiation processes discussed are distinguished from each other using the names "ambient-turbulence initiating mechanism" for the original process and "thrust-based initiating mechanism" for the process identified herein.

II. OVERVIEW OF THRUST-BASED INITIATION PROCESS

A. Negligible Engine Trust

When engine thrust is negligible, the lift-generated wake shed by the wing of the aircraft rolls up into a vortex pair that can be approximated by two-dimensional (2-D) inviscid theory (ref. 16). After the wake has rolled up, three-dimensional (3-D) time-dependent deformations of the lift-generated vortex pair come about by motions of the aircraft or by disturbances from the atmosphere. As indicated in figure 1, when engine thrust is negligible the flow-through exhaust streams of the engines become a part of the rolled-up vortex wake. Any turbulence in the atmosphere is then immediately effective in bringing about wave-like distortions in the vortex filaments because they are in intimate contact with any non-uniformities in the atmosphere near the flight path of the aircraft. The figure is taken from an earlier paper (ref. 42) to display qualitative computations of the roll-up process when the exhaust streams from the engines have about the same velocity as that of the free stream; e.g., during approach to an airport runway. The boundaries of the streams through each of the two engines are each marked by 20 small circles in order to identify how the streams from engines at idle are assimilated into the structure of the vortex pair. The span loading on the wing is designed for minimum weight and lift-induced drag for a specified span of the wing.

The reason for presentation of the computations in figure 1 is to call attention to the fact that, when engines have negligible thrust, the rolled-up vortex wake (round filled symbols) is in immediate and intimate contact with any nearby turbulence eddies present in the atmosphere. This situation is assumed in the ambient-turbulence–based theory for the long-wave instability (refs. 1–3). It was this theory that was simulated and confirmed by experiments conducted in water tow tanks (refs. 19–28).

B. Robust Engine Thrust

When engine thrust is robust, the hot and energetic exhaust streams slow and spread by entrainment of air because of mixing with the cold stationary air of the atmosphere. The enlargement of the wake by entrainment and slowing of the exhaust streams is simulated in figure 2 using active point-source distributions, shown as open circles. The vortex wake (shown by filled circles) now rolls up inside a shroud composed of fluid elements marked by open circles and by fluid emitted from the sources and not marked. The lift-generated, or vortex part, of the wake is now shielded by exhaust gases

from any ambient turbulence in the vicinity of the wake. As a consequence, distortion of the vortex filaments by any turbulence in the atmosphere is cushioned, and not likely to initiate the long-wave instability. If the long-wave instability is to be initiated, it must be initiated by some other mechanism. In each of the figures, the descending vortex pair is formed by the two largest accumulations of point vortex markers (filled circles). At $x/b_o = 100$, the grouping of point vortices near the bottom of the exhaust wake makes up most of the circulation in the filament pair. The other point vortices form the outer layers of the vortex pair. The purpose of figure 2 is to show that, at $x/b_o = 25$ and beyond, exhaust gases form a shield around the vortex part of the wake to reduce the likelihood that ambient turbulence will initiate the long-wave instability.

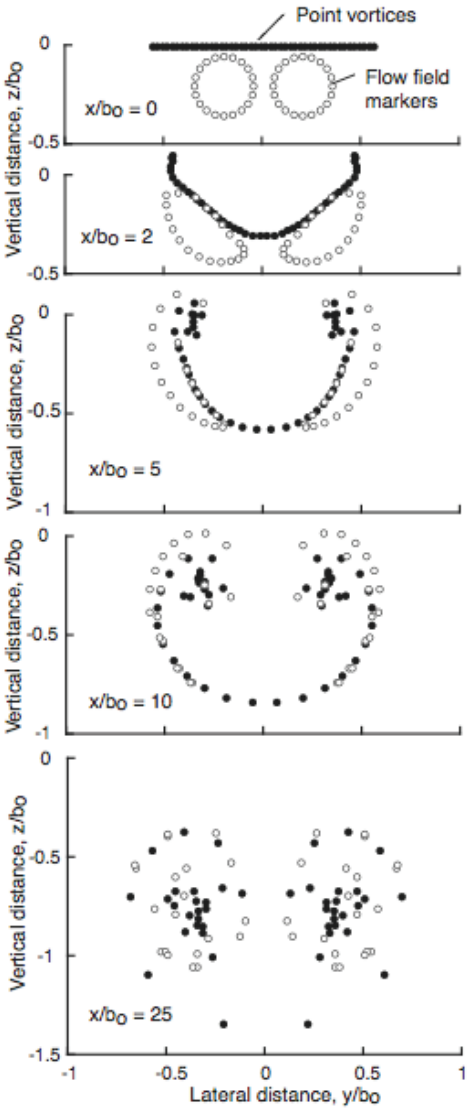

Figure 1. Qualitative computation of assimilation of engine flow-through streams into rolled-up vortex wake at various distances behind generating aircraft (engine thrust is negligible) (ref. 42).

It is suggested here that when jet-engine–thrust levels are robust like those used during takeoff, climb, and cruise, and possibly also during short periods of time where intermittent thrust is used to adjust the velocity or altitude of an aircraft on approach to a runway (refs. 38–40), a thrust-based mechanism initiates the instability. Observations indicate that the process is more complicated than the mechanism based on ambient turbulence. That is, the thrust-based initiation mechanism begins with the development of an array of circumferential vortex rings in the shear layer between each engine-exhaust stream and the surrounding stationary atmosphere. The individual exhaust streams and their shear-layer vortex arrays then merge over time to form a single exhaust stream with a single array of irregularly shaped vortex loops at the interface between the energetic part of the exhaust stream and the atmosphere—i.e., in the region just outside of the region occupied by open circles illustrated in figure 2.

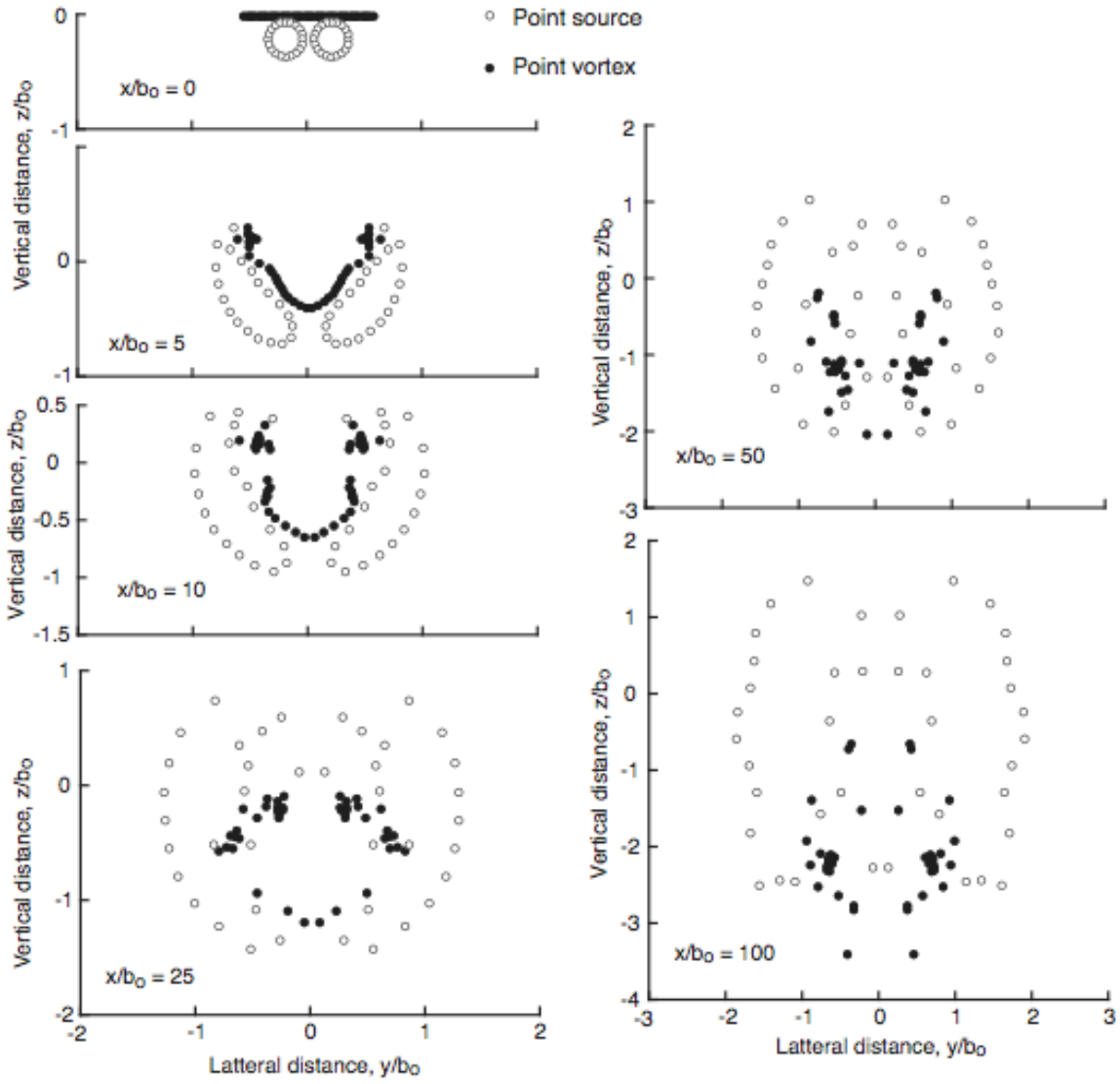

Figure 2. Qualitative computation of formation of shield composed of engine-exhaust products (open circles) around the vortex wake (filled circles) when engine thrust is robust (ref. 42).

Observations at cruise altitudes show that the vortex filaments remain straight and without waves along their length as they descend. Unfortunately, the computational method used to produce figures 1 and 2 is not able to simulate the effect of atmospheric turbulence on the vortex filaments, nor how exhaust products might shield the vortex pair from the turbulence. However, when the pair of vortex filaments has descended far enough to reach the vicinity of the bottom of the shear-layer vortex array, the in and out velocity fields induced by the array of circumferential shear-layer vortices around the merged and distorted jet-engine–exhaust streams generate a series of sinusoidal waves along the vortex pair. Because the wavelengths of the waves (or loops) formed are too short for use by the long-wave instability, the relatively uniform set of short waves induced by the shear-layer vortex array is re-formed into a set of longer wavelengths that then lead to linking of the vortex pair to form closed loops of vortex filaments that decompose the organized structure of the wake. The re-formation process from short to longer wavelengths may be about the same as when vortex wakes encounter ambient turbulence of smaller wavelengths in the atmosphere (as derived by Crow and Bate, ref. 3), or it may be a formation process whereby short loops first form and then merge to form loops of longer wavelength that are acceptable for the linking process. Thereafter, either process appears to be able to cause the re-formed waves to grow in amplitude until the two filaments link to form large irregularly shaped vortex loops that decompose the entire lift-generated wake shed by the aircraft.

III. OBSERVATIONS AND PHOTOGRAPHS OF THRUST-BASED INITIATION

A. Overview

At cruise altitudes, the atmosphere is often at a temperature below –40° F (–40° C) with a humidity level above 40%. When these conditions are present, the water vapor in jet-engine–exhaust streams freezes into small ice crystals as the hot, moist exhaust gases mix with the cold, ambient atmosphere to form what is referred to as a condensation trail. The light scattering characteristics of the ice crystals make it possible to observe much of the dynamics, decomposition, and decay of lift-generated wakes for an improved understanding of how lift-generated vortex wakes redistribute themselves at cruise altitudes as a function of time (refs. 12–17).

Over the years the author has taken numerous photographs of condensation trails (ref. 17). Good candidate photographs were taken as they appeared in the field of view of the observer/photographer even though the conditions for viewing and the orientation of condensation trails at cruise altitudes were often not ideal. Not all wakes produce a condensation trail, even though the temperature of the atmosphere at cruise altitudes is usually well below the required temperature of –40° F (–40° C). When the humidity of the atmosphere is below 40%, the ice crystals formed by the mixing of exhaust products with cold, ambient air evaporate or sublime and do not persist. When ice crystals form in marginal numbers, only the outer parts of the jet-exhaust streams are visualized. When the humidity at cruise altitudes is well above 40%, large quantities of ice crystals form to visualize both the shear-layer vortex system and the lift-generated vortex wake for an hour or more. Unfortunately, when ice crystals form in large numbers, many of the internal features of the wake are obscured. A satisfactory history of wake dynamics can then be obtained only by making a large number of observations that include those with a bare minimum of condensate to those where there is too much

condensate. In addition, the viewing angle of a condensation trail is often not the one desired because the observations and photographs are made from the ground and not from a nearby aircraft. An attempt was made to take photographs when the viewing angle was around 45° or less. Not only was it hard to keep such a rule, but the rule was aggravated by the fact that the viewing angle changes as the aircraft passes the viewing station.

The photographs were taken as they appeared in the sky—neither plan nor side views—and an estimate of the viewing angle was not recorded because the author was most interested in getting good pictures. Uncertainty exists, therefore, as to the viewing angle, the relative locations of wake components, and processes in addition to the aircraft type. As a result, the author's interpretation of some of the details in the pictures presented may later be shown to be incorrect when improved photographs are obtained by use of aircraft flying near the wakes being explored. However, it is believed that the process described herein for the initiation of the long-wave instability when engine thrust is robust is basically correct. Because the photographs were taken under dynamic conditions, very little information is available about the circumstances for a given photograph.

In spite of data-taking difficulties, it is believed that the photographs presented support the thrust-based initiation process described herein. The photographs were chosen to provide pictures of the condensation trails that were related to the time history of the shapes of the exhaust streams and of the vortex pair because they were the best available, even though not ideal. Most of the pictures presented have had their contrast enhanced a small amount to improve identification of various flow-field components. The flight direction exhibited in all of the figures has the aircraft flying from the right to the left for ease of interpretation.

B. Shear-Layer Vortex Mesh Around Exhaust Streams of Jet Engines

As a reminder, two vortex systems exist behind aircraft flying at cruise altitudes (figure 3). The first is the lift-generated vortex pair that trails from the wing of the aircraft and moves downward with time in response to the self-induced velocity field between the two equal and opposite vortices in the pair. The second is the shear-layer vortex system that begins just behind the aircraft to form at the interface between each jet-engine–exhaust stream and the nearly stationary atmosphere. The shear-layer vortex system is first illustrated in this section by using photographs of several condensation trails at a time when conditions are marginal for formation of ice crystals. Therefore, only the shear-layer vortices are visualized, and the remainder of the exhaust system is transparent. In the photographs, the lift-generated vortex pair is not visualized by ice crystals, because it is believed that the two vortices are surrounded by exhaust gases and not yet by a mixture of atmosphere and exhaust gases.

Condensation trails begin almost immediately behind the wake-generating aircraft as exhaust streams exit from the jet engines that propel the aircraft. At first, only the outer parts of the exhaust streams are visible, but more becomes visible as the exhaust mixes with the ambient atmosphere for formation of ice crystals that serve as the fluid markers. For this reason, photographs are first presented in figure 3 for a two-engine aircraft, and in figure 4 for a four-engine aircraft to show the shear-layer vortex structures that form around the jet-engine–exhaust streams as they trail behind aircraft. In both cases the jet-engine–exhaust streams slow relative to the atmosphere and then merge

so that their radii grow to eventually become much larger than the wingspan of the wake-generating aircraft.

Figure 3 shows that the shear-layer vortex arrays or meshes that surround the two engine-exhaust streams first appear to spread at a total angle of about 4°, and then decrease to a spreading angle of about 1° or less. The reason for changes in the apparent rate of spreading of the jet streams is that the visible ice crystals do not mark the exteriors of the exhaust streams, but instead mark where ice crystals have survived. That is, ice crystals first form at the interface between each exhaust stream and the atmosphere and then gather around each segment of the vortex-filament mesh as the swirling flow of each vortex segment mixes hot, moist air from the inside edge of each jet stream outward into the cold, ambient atmosphere where ice crystals form. If conditions for condensation are marginal, the ice crystals outside of the exhaust streams and in the shear-layer vortex arrays sublime and disappear, rather than remaining visible. Therefore, as the jet streams age their cross-sectional size first appears to grow as it mixes with the atmosphere, and then appears to shrink in cross-sectional size because the ambient air has a low humidity that causes the ice crystals to sublime. The

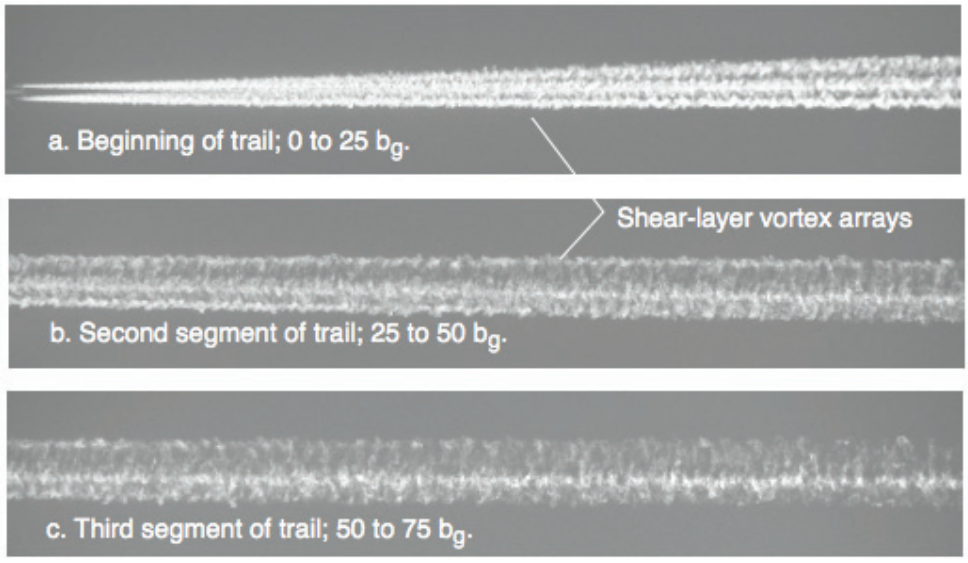

Figure 3. Diagonal view of condensation trail displayed by jet-engine–exhaust streams of two-engine aircraft. Small amounts of condensate visualize shear-layer vortex arrays around both exhaust streams in part (a), and their merger in part (c) as ice crystals sublime.

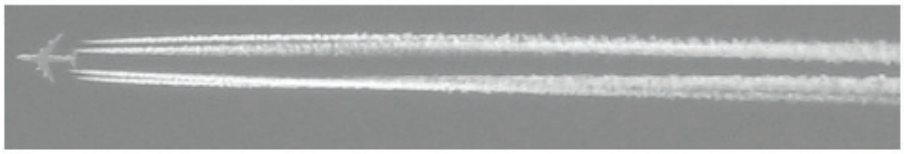

Figure 4. View of condensation trail from aircraft with 4 jet engines as the two streams from engines on each side of the aircraft rotate about each other because of the action of the vortex wake and then merge; the view is about 0 to 10 b_g. Merger of port and starboard jet streams does not occur until about 100 b_g after aircraft passage. Lift-generated vortices are not visible.

last picture in figure 3 shows the exhaust streams as shrinking in size, but not yet completely gone. As a consequence, the outside of the vortex filaments that visualize the exhaust trails shown in figures 3 and 4 do not include all of the gases that contain exhaust products, so they do not necessarily represent the outside surfaces of all of the mixture of engine exhaust and ambient air.

Although the shear-layer vortex arrays are sometimes observed as a neat sequence of coaxial vortex rings around each exhaust stream, the patterns most often observed consist of a somewhat random diagonal system of vortex segments that are tied together like a network of stretched strings around a long sausage, as photographed in figures 3 and 4. As distance behind the aircraft increases, the multiple exhaust streams mix with the atmosphere and with each other to form a single exhaust stream with a single shear-layer vortex array around its exterior. The reduced velocity in the merged exhaust stream causes the shear-layer vortex mesh to be compressed in the streamwise direction and to become enlarged in cross-sectional size.

The segments of irregularly shaped vortex rings around the combined exhaust streams then become more evenly spaced, and more nearly perpendicular to the axis of the combined jet stream, so that the re-formed mesh pattern more closely approximates coaxial vortex rings (fig. 3c). Although the overall structure is still complex, the circumferential shear-layer vortex lines appear to become more evenly spaced and nearly transverse to the flight direction. As a result, the shear-layer vortex system has developed the capability to initiate regularly spaced waves along the lift-generated vortex-filament pair to provide the disturbances needed to carry out the initiation of the long-wave instability. Overlap of exhaust streams as they spread and as the viewing angle changes makes it difficult to interpret some features in the pictures. Of importance is the fact that the individual jet streams grow in cross-sectional size, and they appear to overlap and then merge with distance behind the wake-generating aircraft.

C. From Roll-Up Through Linking of Vortex Pair

As illustrated in figures 3, 4, and 5a, a shear-layer vortex array first forms around each jet-engine–exhaust stream almost immediately after aircraft passage. In figures 5b and 5c, the shear-layer vortex arrays are visible in the photographs as diffuse, nearly vertical striations in the middle and upper part of the wake. It should be noted that the upper part of the wake has about doubled in depth between figures 5b and 5c. Also shown in both of the figures as thicker, nearly straight white lines is the lift-generated vortex pair first near the bottom of the combined jet-engine–exhaust streams and their shear-layer vortex array and then at the bottom (fig. 5c). In figure 5d, the vortex pair is at the inside bottom of the flow field just inside of the vortex array where the vortex pair has become distorted into a sequence of in-phase waves that appear as segmented humps. That is, when the pair of vortex cores or filaments approaches the inside of the bottom of the shear-layer vortex array that surrounds the exhaust condensate, waves of nearly the same wavelength form along the filament pair (figs. 5c and 5d). It is the up- and downward velocity field between the shear-layer vortices at the bottom of the shear-layer vortex array that induces these waves on the vortex filaments. The amplitude of these short waves grows rapidly at first and then stops growing because of the limited depth of the vertical velocity field inside the shear-layer vortex array.

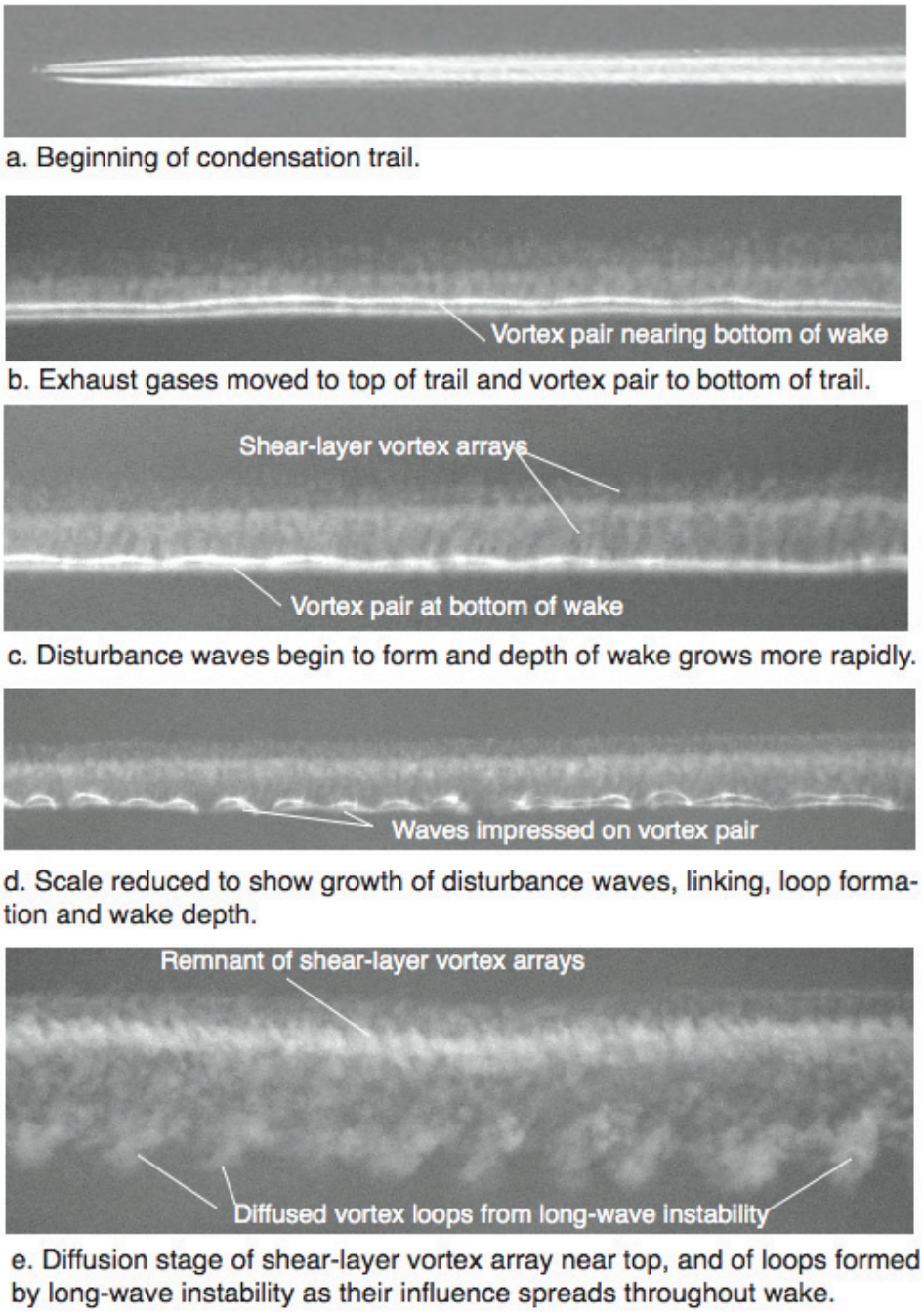

Figure 5. Photographs of progress of structure of condensation trail from when first shed by aircraft to shortly after linking and loop formation of lift-generated vortices.

Figure 5e presents a view of the closed loops of decomposing and diffusing lift-generated vortex segments that have formed into irregularly shaped vortex loops by the long-wave instability. The lower lobes of diffuse condensate indicate where the loops of vortex filaments have their greatest downward extension. The upper parts of the shear-layer vortex array are indicated by a closely spaced sequence of white-filled ellipses. The lower part of the wake consists of the diffuse,

irregularly shaped vortex loops that were formed by linking of lift-generated vortices brought about by the long-wave instability. The vortex loops have lost their crisp appearance by becoming diffuse, so they appear as long puffs of condensate loops rather than small-diameter filaments (fig. 5e). In the cases observed, the ratio of the spacing between shear-layer vortices and the loops formed by the long-wave instability is consistently somewhere between 3 and 4 (figs. 5e and 6b).

The spacing between shear-layer vortices is apparent in both figures 5 and 6, but is most clearly defined in figure 6b. The vortex loops that have formed by vortex linking have had their structure changed from straight-line filaments to filaments with waves, and from continuous filaments to closed loops of vortex filaments that then become diffused, smeared out, or destroyed by actions of the vortex loops formed by the long-wave instability. Figures 5e and 6b also indicate the approximate shapes and spacing between the vortex loops that are formed after the two vortices in the lift-generated vortex pair have linked. The ratio of distance between successive shear-layer vortices and vortex-loop formations consistently appear to be between three and four shear-layer vortex spacings for each single loop of the long-wave instability. All of the condensation trails observed exhibited the same spacing rule.

Also shown in figures 5e and 6b is a curious characteristic where the loops formed by the long-wave instability slope to the right. It is believed that part of the reason for the slanting shape is that the loops are moving downward as they age. Therefore, because the older part (the left part) had a head start at descending motion, it enters the stationary part of the atmosphere well before the upper part. Another reason for the slanted form is that as the jet-engine–exhaust streams have merged into a single stream that broadens as their velocity slows relative to the surrounding atmosphere, fluid

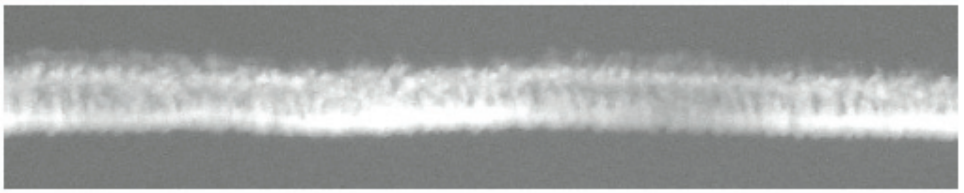

a. View of orderly shear-layer vortex array along condensation trail just before long-wave instability is initiated.

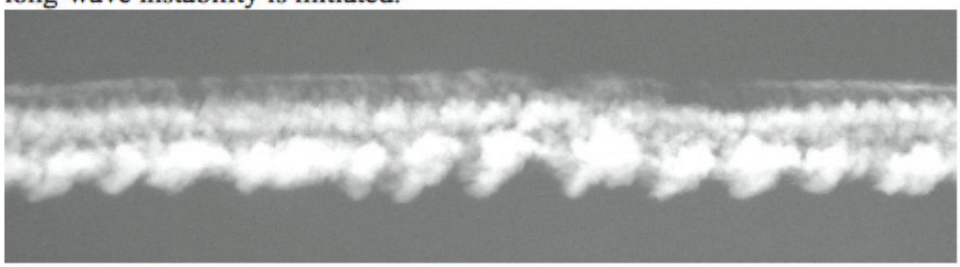

b. View of same condensation trail after linking and loop formation has occurred.

Figure 6. Comparison of spacings between shear-layer vortices with spacings between loops of vortex filaments that are in the process of diffusing.

elements within the center part of the wake and inside or next to the rearward-moving exhaust stream continue to move rearward. In contrast, fluid elements (e.g., loops of vortex filaments) that are near the outside of the exhaust stream are almost stationary relative to the atmosphere. As a consequence, those parts of the exhaust streams move the flow field rearward, causing the vortex loops to slant (figs. 5 and 6).

IV. TIME-TO-LINKING ESTIMATE OF LINKING

The Crow-Bate theory assumes that the formation of disturbance waves for initiation of the long-wave instability begins almost immediately after aircraft passage. The assumption is a good one because the pair of vortex filaments shed by an aircraft is in immediate contact with the atmosphere and its turbulent eddies when engine-thrust levels are negligible (fig. 1). This is not the case when disturbance waves are initiated on vortex filaments by the shear-layer vortex arrays generated by robust jet-engine–exhaust streams. In those cases, as shown in the foregoing figures, the vortex pair must first travel from about the vertical center of the wake (or condensation trail) down to the bottom of the wake where the bottom of the array of shear-layer vortices resides. Thereafter, the time interval required for amplification and reassembly of disturbance waves into those that progress into the linking and loop formation stages of the instability should be about the same as the Crow-Bate estimate for vortex linking (ref. 3). Therefore, the Crow-Bate estimate (fig. 7) for a time to linking after wake generation by disturbance waves that consist of ambient turbulence is used as a basis for a time-to-linking estimate that takes place when the disturbance waves are generated by jet-engine–exhaust shear-layer vortices.

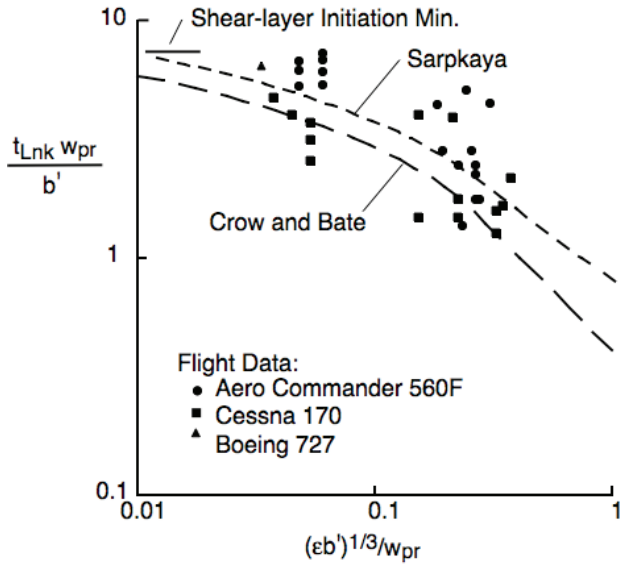

Figure 7. Minimum increase in time to linking when long-wave instability is initiated by shear-layer vortex array.

The estimate for the downward travel time of the vortex pair from the original location just behind the generating aircraft down to the vicinity of the bottom of the shear-layer vortex array is based on two parameters. The first is an estimate for the maximum travel velocity of the vortex pair, and the second is an estimate for the shortest likely travel distance from where the vortex sheet is generated down to near contact level at the bottom of the inner part of the flow field of the shear-layer vortex array. Those values yield an estimate for the minimum amount of time needed for the vortex pair to move from the elevation where the vortex pair was generated down to roughly where the bottom of the wake is located at the time that the vortex wake arrives.

The derivation begins with an estimate for the maximum self-induced downward travel velocity of a vortex pair as given by

$$w_{pr} = -|\Gamma_o|/2\pi b' \tag{1}$$

where it is assumed that the vortex strength, $|\Gamma_o|$, and the spanwise distance between the centers of the vortices in the pair, b', are the same as when the wake was first generated by the aircraft. The estimate made by equation (1) yields the maximum self-induced downward velocity because the strength of each vortex filament is assumed to be the same for the entire downward trip as when first generated by the roll-up of the vortex sheet shed by the wing. Those values were chosen even though some of the circulation has been stripped away from around the vortex centers and has been moved to the top of the wake. The reduction of the circulation content of each vortex is made by removal of some of the layers of vorticity in the outer layers of the vortices to the top of the wake by the swirling action of the opposite vortex in the pair. Turbulence in the exhaust streams of the jet engines also tends to spread the vortices. These processes tend to reduce the circulation content and thereby increase the downward travel time of the pair of vortex filaments or cores. It is also assumed that the separation distance, b', between the two vortices in the pair is unchanged by any of the foregoing processes from its initial value of about $b' \approx \pi b_g/4$.

Because the cross-sectional size of the wake is increasing with time as the vortex pair descends, the travel distance of the vortex pair is also uncertain. For the purposes of the present approximate estimate of travel time, the travel distance (one-half of the wake diameter) is estimated as somewhere between 2 b_g and 3 b_g. It is argued that the jet-engine–exhaust streams expand from their original diameter to about 3 b_g, or perhaps more. Observations of wake sizes at the time of arrival of the vortex pair at the bottom of the shear-layer vortex array appear sometimes to be as much as or more than 4 b_g in diameter. Because the smallest value for travel time is desired, the downward travel distance of the pair is taken as 1.5 b_g. An estimate for the minimum travel time of the vortex pair is then given by:

$$\Delta t_{Dwn} = 1.5\, b_g/w_{pr} = 1.5\, b_g/(|\Gamma_o|/2\pi b') \tag{2}$$

The assumed circulation content of each vortex in the pair can be converted to aircraft parameters by using two equations for the lift on the wing of the wake-generating aircraft. Because aircraft flying at cruise altitudes are in steady level flight, the weight of the aircraft is the same as the lift produced by the wing of the aircraft, or

$$Wt = L = \rho U_\infty |\Gamma_o| b' \tag{3}$$

The lift is also given by

$$L = C_{Lg} S \rho U_\infty^{\,2}/2 \tag{4}$$

The dimensionless circulation may then be written as

$$|\Gamma_o|/b_o U_\infty = 2C_{Lg}/\pi AR_g \tag{5}$$

so that the self-induced downward velocity of the lift-generated vortex pair may be written as

$$w_{pr}/U_\infty = -4C_{Lg}/\pi^3 AR_g \approx -0.0184 \tag{6}$$

for all similar aircraft whose lift coefficient is about 1.0 and wing aspect ratio is about 7. An estimate for the time required for the vortex pair to descend from the center of the wake down to the bottom of the wake where disturbance waves are impressed on the filaments is then given by

$$\Delta t_{Dwn} = 1.5\, b_g/w_{pr} \approx 14 \text{ s} \tag{7}$$

when the wake-generating aircraft has a wing span of 200 ft and is flying at about 800 ft/s. In comparison, observed times are difficult to determine visually from the ground, but appear to vary from about 20 s to 100 s.

In terms of the Crow-Bate time-to-linking parameter, the downward travel time may be written as

$$\Delta\tau_{Dwn} = \Delta t_{Dwn} w_{pr}/b' = 1.5\, b_g/b' = 1.91 \approx 2 \tag{8}$$

When the downward travel time of the vortex pair is added to the Crow-Bate estimate of 6 units (for when the ambient turbulence is small), the sum yields a total value of around 8 units. A short horizontal line is shown in figure 7 for shear-layer thrust initiation, which is in fair agreement with the data point for the B-727.

V. CONCLUSIONS

It is well known that the long-wave instability of a vortex pair is the aerodynamic mechanism that decomposes and spreads lift-generated vortex wakes more rapidly than any other mechanism. It has also usually been assumed that turbulence in the atmosphere is the initiation mechanism for the long-wave instability. Theoretical and experimental studies of the growth of the long-wave instability have been confirmed by experiments in water tow tanks when engine thrust is absent or at low levels.

However, when engine-thrust levels are robust as during takeoff, climb, and cruise, and during periods of flight-path adjustments during approach to a landing, a thrust-based mechanism initiates the long-wave instability in the lift-generated vortex pair. Robust engine thrust first generates an array of vortices in each of the shear layers between the engine-exhaust streams and the atmosphere. Shortly after generation, the self-induced velocity field of the lift-generated vortex pair moves the exhaust gases and their vortex arrays from near the bottom of the wing around to the sides and the top of the wake. The vortex pair may then be shielded from any turbulence in the ambient atmosphere near the aircraft wake. During this time, the lift-generated vortex pair moves downward to the bottom of the wake, where it encounters the up and down velocity field of the combined shear-layer vortex arrays, which initiates the long-wave instability.

The photographs provided illustrate and support the thrust-based initiation process described herein. Unfortunately, the photographs of condensation trails at cruise altitudes were taken from the ground at a variety of different viewing angles and condensation conditions. As a consequence, the photographs are somewhere between side views and views from directly below the condensation trail, making it difficult to discern the exact detailed dynamics within the wake of the aircraft. Although the uncertainty in the interpretation of the dynamics within the wake is bothersome, the evidence is clear that the long-wave instability is initiated by the thrust-based mechanism described here and not by ambient turbulence. It is also obvious that the velocity field at the bottom of the shear-layer vortex array that surrounds the unified streams of the engines does provide the wave-initiation process. Because some of the details of the thrust-based initiation process are vague, it is recommended that further experimental evidence be obtained by means of photographs taken of the process from an aircraft flying beside, from beneath, and from above condensation trails to more fully describe the thrust-based initiation process and to provide a more exact description of its details. An improved theoretical analysis is also needed for the process to improve the understanding of and accuracy for the estimate of the time for the process.

APPENDIX:
CONFIRMATION OF THEORY BASED ON AMBIENT TURBULENCE

A. Overview

This appendix presents an overview of the experimental studies that were carried out to confirm the ambient-turbulence model developed by Crow and Bate for the initiation and dynamics of the long-wave instability in a vortex pair. It is found that the experiments conducted in water tow tanks on the basics of the long-wave instability have a small amount of scatter. That fact helps to demonstrate the accuracy of the Crow-Bate model and the fidelity of the experimental work on matching the ambient-turbulence initiation process assumed in the theory. The larger amount of scatter in the flight data presented in the Crow-Bate paper is not discussed because, as explained in the paper, it is now believed that the long-wave instability is not initiated at cruise altitudes by the ambient-turbulence initiation process but by a thrust-based initiation process. Therefore, the discussion presented here treats only the confirmation of the ambient-turbulence–based model derived by Crow and Bate. Confirmation of the theoretical model for the long-wave instability when initiated by ambient turbulence is important for an understanding of the dynamics of the long-wave instability and for an estimate of the time needed for its execution when initiated by the shear-layer vortex arrays produced by robust engine thrust.

The theoretical representations derived by Crow and Bate indicate that the preferred wavelengths for vortex linking by the ambient-turbulence process range from about 4 b’ to about 10 b’ ($b' \approx \pi b_g/4$). After initiation, the planes of oscillation of the growing waves on the two filaments in the vortex pair each rotate in a direction opposite to that of the swirl direction in the vortex itself as the wave amplitude grows (refs. 10 and 11). The increase in wave amplitude and the rotation of the two wave planes combine to move the wave troughs inboard towards each other until the troughs are close enough to each other to link across the center plane of the flow field. The linking process causes the vortex filaments to form irregularly shaped loops of vortex filaments that continuously and rapidly reform their shape to bring about large-scale fluid motions that decompose the originally well-organized flow field of the vortex pair. The instability has then changed the hazard posed by the wake to penetrating aircraft from a coherent over-powering rolling moment to an incoherent random bumpy ride (ref. 16).

B. Parameters Used

The parameters used to describe the characteristics of the long-wave instability (refs. 1–3) include the eddy-dissipation rate, ε, of the turbulence in the fluid where the lift-generated wake is embedded, and the time after aircraft passage, t_{Link}, at which linking occurs across the centerline of the wake by the two vortex filaments. These two parameters are made dimensionless by combining them with b’, the initial spanwise distance between the centers of the two vortices in the pair, and w_{pr}, the initial estimated self-induced downward velocity of the vortex pair. The quantity b’ is assumed to be related to the span of the wake-generating aircraft by $b' \approx (\pi/4)b_g$, and w_{pr} is taken as $\Gamma_o/2\pi b'$, where Γ_o is the circulation bound in the wake-generating wing at its centerline. Two dimensionless

parameters, a time-to-linking parameter, $[t_{Lnk}w_{pr}/b']$, and a turbulence parameter, $[(\varepsilon\, b')^{1/3}/w_{pr}]$, are then used to compare the Crow-Bate theory for time to linking with measured data (fig. 7).

C. Vortex-Linking Experiments in Water Tow Tanks

Experimental studies of the characteristics of the long-wave instability of a vortex pair were carried out in water tow-tank test facilities (refs. 19–28) to confirm the theoretical analyses (refs. 1–3) and to better understand the relationship between the structure of the turbulence in the ambient fluid and the time to linking of the two vortices in the pair, t_{Link}. The water tow tank is the ideal instrument for testing the analysis of Crow and Bate because the characteristic parameters, ε, b', w_{pr}, and t_{Lnk}, can all be readily generated and measured reliably in a water tow tank. A broad range of turbulence levels were generated in the ambient fluid by using different grid sizes that were towed through the water before each test run with a lifting wing to generate various levels and scales of turbulence. The tow tank does have the disadvantages of being at small scale and small Reynolds numbers, but the cost of many laboratory measurements is small compared with even a small number of flight tests, where control and measurement of important parameters are difficult—if not impossible—to obtain.

The large number of data points obtained in water tow tanks are not shown in figure 7 because their large number obscures the two theoretical curves presented. Instead, only the theoretical curves developed by Crow and Bate (ref. 3) and by Sarpkaya (ref. 23) are shown because the experimental data are distributed closely around the theoretical curves to provide a convenient average of all of the tow-tank data taken by Sarpkaya (refs. 19 and 22–24) and by the staff of the Northwest Research Associates (refs. 25–28). The averaged tow-tank data and Sarpkaya's recommended curve are noted to have about the same shape as and to be just above the curve predicted by the theory of Crow and Bate (ref. 3). The results obtained by Liu (refs. 20 and 21) confirm the results of the Crow-Bate analysis and provide flow-field visualization and other information on the decomposition of vortex wakes that are brought about by ambient turbulence, stratification, and the proximity of the ground plane.

Even though the tow-tank data are not in exact agreement with the theoretical predictions of Crow and Bate, the data confirm the predicted trends and indicate that proper attention to the details of the flow-field structure in the development of the long-wave instability does produce data that have a small amount of scatter and are in good agreement with theory. A negative aspect of the data taken in water tow tanks is that, because of its small scale and the confinement by the walls of the test tank, it may have a systematic change in the level of linking times from what might be found if larger sizes of water tow tanks and turbulence-generating grids had been used in the experiments. Such a conjecture is suggested by the observation that the largest grid size used in the various tow tanks is only large enough to produce turbulence eddies of wavelength sizes up to about 4 b', whereas the optimum wavelength for stimulation and support of the instability is 8.6 b'. Therefore, if larger grid sizes had been used (a larger facility would have been required) to generate turbulence, the measured linking times might have been in complete agreement with the theoretical estimates made by Crow and Bate (ref. 3). None of the experiments in water tow tanks simulated the action of jet-exhaust streams for a simulation of vortex wakes at cruise altitudes.

REFERENCES

1. Crow, S.C.: Stability Theory for a Pair of Trailing Vortices. AIAA J., vol. 8, no. 12, Dec. 1970, pp. 2172–2179.
2. MacCready, P.B., Jr.: An Assessment of Dominant Mechanisms in Vortex-Wake Decay. Aircraft Wake Turbulence and Its Detection, 1st Edition. Olsen, J.H.; Goldburg, A.; and Rogers, M., eds., Plenum Press, 1971, pp. 289–304.
3. Crow, S.C.; and Bate, E.R., Jr.: Lifespan of Trailing Vortices in a Turbulent Atmosphere. AIAA J. Aircraft, vol. 13, no. 7, July 1976, pp. 476–482.
4. Tombach, I.H.: Observations of Atmospheric Effects on Vortex Wake Behavior. AIAA J. Aircraft, vol. 10, no. 11, Nov. 1973, pp. 641–647.
5. Widnall, S.E.; Bliss, D.; and Zalay, A.: Theoretical and Experimental Study of the Stability of a Vortex Pair. Aircraft Wake Turbulence and Its Detection, 1st Edition. Olsen, J.H.; Goldburg, A.; and Rogers, M., eds., Plenum Press, 1971, pp. 305–338.
6. Olsen, J.H.: Results of Trailing Vortex Studies in a Towing Tank. Aircraft Wake Turbulence and Its Detection, 1st Edition. Olsen, J.H.; Goldburg, A.; and Rogers, M., eds., Plenum Press, 1971, pp. 455–472.
7. Condit, P.M.; and Tracy, P.W.: Results of the Boeing Company Wake Turbulence Test Program. Aircraft Wake Turbulence and Its Detection, 1st Edition. Olsen, J.H.; Goldburg, A.; and Rogers, M., eds., Plenum Press, 1971, pp. 473–508.
8. Bilanin, A.J.; and Widnall, S.E.: Aircraft Wake Dissipation by Sinusoidal Instability and Vortex Breakdown. AIAA Paper 73-107, 1973.
9. Donaldson, C. duP.; and Bilanin, A.J.: Vortex Wakes of Conventional Aircraft. Advisory Group for Aerospace Research and Development, AGARDograph no. 204, May 1975.
10. Rossow, V.J.: Wake Hazard Alleviation Associated with Roll Oscillations of Wake-Generating Aircraft. AIAA J. Aircraft, vol. 23, no. 6, June 1986, pp. 484–491.
11. Rossow, V.J.: Prospects for Destructive Self-Induced Interactions in a Vortex Pair. AIAA J. Aircraft, vol. 24, no. 7, July 1987, pp. 433–440.
12. Lewellen, D.C.; and Lewellen, W.S.: Large-Eddy Simulations of the Vortex-Pair Breakup in Aircraft Wakes. AIAA J., vol. 34, no. 11, 1996, pp. 2337–2345.
13. Lewellen, D.C.; and Lewellen, W.S.: The Effects of Aircraft Wake Dynamics on Contrail Development. J. Atmos. Sci., vol. 58, 2001, pp. 390–406.
14. Quackenbush, T.R.; Teske, M.E.; and Bilanin, A.J.: Dynamics of Exhaust Plume Entrainment in Aircraft Vortex Wakes. AIAA Paper 96-0747, 1996.
15. Gerz, T.; and Ehret, T.: Wake Dynamics and Exhaust Distribution Behind Cruising Aircraft. Advisory Group for Aerospace Research and Development, Proc. AGARD Symposium, Trondheim, Norway, CP-584, 1996, pp. 35.1–35.12.

16. Rossow, V.J.: Lift-Generated Vortex Wakes of Subsonic Transport Aircraft. Progress in Aerospace Sciences, vol. 35, no. 6, Aug. 1999, pp. 507–660.

17. Rossow, V.J.; and James, K.D.: Overview of Wake-Vortex Hazards During Cruise. AIAA J. Aircraft, vol. 37, no. 6, 2000, pp. 960–975.

18. Bobylev, A.V.; Vyshinsky, V.V.; Soudakov, G.G.; and Yaroshevsky, V.A.: Aircraft Vortex Wake and Flight Safety Problems. AIAA J. Aircraft, vol. 47, no. 2, 2010, pp. 663–674.

19. Sarpkaya, T.; and Daly, J.J.: Effect of Ambient Turbulence on Trailing Vortices. AIAA J. Aircraft, vol. 24, no. 6, June 1987, pp. 399–404.

20. Liu, H.-T.; and Srnsky, R.A.: Tow Tank Simulation of Vortex Wake Dynamics. Hallock, J.N., ed., Proceedings Aircraft Wake Vortices Conference Volumes 1 and 2, U.S. Dept. of Transportation, Federal Aviation Admin., DOT/FAA/SD-92/1.1, DOT-VNTSC-FAA-92-7.1, Washington, D.C., Oct. 29–31, 1991, pp. 32-1-26.

21. Liu, H.-T.: Effects of Ambient Turbulence on the Decay of a Trailing Vortex Wake. AIAA J. Aircraft, vol. 29, no. 2, March–April 1992, pp. 255–263.

22. Sarpkaya, T.: Decay of Wake Vortices of Large Aircraft. AIAA J. Aircraft, vol. 36, no. 9, Sept. 1998, pp. 1671–1679.

23. Sarpkaya, T.: New Model for Vortex Decay in the Atmosphere. AIAA J. Aircraft, vol. 37, no. 1, Jan.–Feb. 2000, pp. 53–61.

24. Sarpkaya, T.; Robbins, R.E.; and Delisi, D.P.: Wake-Vortex Eddy-Dissipation Model Predictions Compared with Observations. AIAA J. Aircraft, vol. 38, no. 4, July–Aug. 2001, pp. 687–692.

25. Robins, R.E.; and, Delisi, D.P.: Potential Hazard of Aircraft Wake Vortices in Ground Effect with Crosswind. AIAA J. Aircraft, vol. 30, no. 2, March–April 1993, pp. 201–206.

26. Robins, R.E.; Delisi, D.P.; and Greene, G. C.: Algorithm for Prediction of Trailing Vortex Evolution. AIAA J. Aircraft, vol. 38, no. 5, Sept.–Oct. 2001, pp. 911–917.

27. Robins, R.E.; Delisi, D.P.; Greene, G. C.: Aircraft Wake Vortex Core Size Measurements. 21st AIAA Applied Aerodynamics Conf., Orlando, Fla., June 23–26, 2003, AIAA 2003-3811.

28. Delisi, D.P.: Laboratory Measurements of the Effect of Ambient Turbulence on Trailing Vortex Evolution. 44th AIAA Aerospace Sciences Meeting and Exhibition, Reno, Nev., Jan. 2006, AIAA 2006-1078.

29. McCready, P.B., Jr.: Turbulence Measurements by Sailplane. J. Geophys. Res., vol. 67, no. 2, March 1962.

30. McCready, P.B., Jr.: Standardization of Gustiness Values from Aircraft. J. Applied Meteorology, vol. 3, no. 8, Aug. 1964, pp. 439–449.

31. McCready, P.B., Jr.; Williamson, R.E.; Berman, S.; and Webster, A.: Operational Application of a Universal Turbulence Measuring System. NASA Contractor Report, NASA CR-62025, Nov. 1965.

32. McCready, P.B., Jr.: Williamson, R.E.; Berman, S.; and Webster, A.: Operational Application of a Universal Turbulence Measuring System. NASA Contractor Report, NASA CR-62025, Nov. 1965.

33. McCready, P.B., Jr.: Operational Application of a Universal Turbulence Measuring System. AMS/AIAA Conf. Aerospace Meteorology, Los Angeles, Calif., March 28–31, 1966, AMS/ AIAA Paper no. 66-364.

34. Department of Defense Handbook, Flying Qualities of Piloted Aircraft, MIL-STD-1797A, June 28, 1995, Appendix A, 4.9.2 Definition of atmospheric disturbance model form, pp. 678–687.

35. Hinze, J.O.: Turbulence, An Introduction to Its Mechanism and Theory. McGraw-Hill Book Co., Inc., 1959, pp. 180–190.

36. Biswas, G.; and Eswaran, V.: Turbulent Flows, Fundamentals, Experiments and Modeling. Narosa Publishing House, New Delhi, India, 2002, pp. 44–58.

37. Rossow, V.J.; and Meyn, L.A.: On Data Scatter in Measured Linking Times for Lift-Generated Vortex Pairs. 46th AIAA Aerospace Sciences Meeting and Exhibit, Reno, Nev., January 7–10, 2008, AIAA-2008-0338.

38. Rossow, V.J.; and Meyn, L.A.: Guidelines for Avoiding Vortex Wakes During Use of Closely Spaced Parallel Runways. 26th AIAA Applied Aerodynamics Conference, Honolulu, Hi., Aug. 18–21, 2008, AIAA 2008-6907.

39. Verma, S.; Lozito, S.; Trot, G.; and Ballinger, D.: Guidelines for Flight Deck Procedures for Very Closely Spaced Parallel Runway Approaches. 27th Digital Avionics Systems Conference, Oct. 26–30, 2008.

40. Verma, S.; Lozito, S.; and Trot, G.: Preliminary Guidelines on Flight Deck Procedures for Very Closely Spaced Parallel Runway Approaches. 16th International Congress of the Aeronautical Sciences, ICAS 2008-574-Verma-7-01-08.

41. Rossow, V.J.: Vortex-Free Flight Corridors for Aircraft Executing Compressed Landing Operations. AIAA J. Aircraft, vol. 43, no. 5, Sept.–Oct. 2006, pp. 1424–1428.

42. Rossow, V.J.; and Brown, A.P.: Effect of Jet-Exhaust Streams on Structure of Vortex Wakes. AIAA J. Aircraft, vol. 47, no. 3, May–June 2010, pp. 1076–1083.